

Electron Transfer Chemistry of Psoralen and Coumarin Derivatives by Means of Radiolytic and Electrochemical Experiments

Tongqian Chen and Matthew S. Platz*

Newman and Wolfrom Laboratories of Chemistry, The Ohio State University, 100 West 18th Avenue, Columbus, Ohio 43210

Marc Robert and Jean-Michel Savéant*

Laboratoire d'Electrochimie Moléculaire, URA CNRS 438, Université Denis Diderot (Paris 7), 2 Place Jussieu, 75251 Paris Cedex 05, France

Andrzej Marcinek, Jacek Rogowski, and Jerzy Gebicki*

Institute of Applied Radiation Chemistry, Technical University, 90-924 Lodz, Poland

Zhendong Zhu and Thomas Bally*

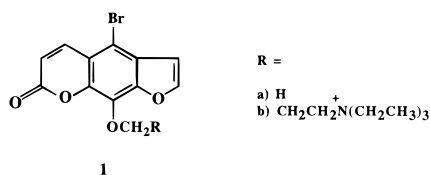
Institute for Physical Chemistry, University of Fribourg, Perolles, CH-1700 Fribourg, Switzerland

Received: October 8, 1996; In Final Form: January 2, 1997[®]

Bromopsoralens and bromocoumarins have been used to sensitize the inactivation of viruses. The bromine substituent increased the antiviral potency of the sensitizer, an effect attributed to cleavage of the C–Br bond of the aromatic radical anion produced by a light-induced electron transfer reaction with nucleic acids. This hypothesis was tested by a detailed mechanistic electrochemical investigation in acetonitrile and *N,N*-dimethylformamide of 5-bromo-8-methoxypsoralen, 8-methoxypsoralen, 3-bromocoumarin, and coumarin. A one-electron reduction process involves the formation of a radical anion, a step coupled with the cleavage of the carbon–bromine bond in the case of the brominated compounds, leading to the formation of an aryl radical moiety and a bromide anion. These experiments were further confirmed by radiolytic preparation coupled with UV–vis detection of the radical anions in glassy 2-methyltetrahydrofuran at 77 K and in ether, acetonitrile, and alcohol solutions at ambient temperature. This allows complete kinetic characterization of the ionic intermediates. The shorter lifetimes obtained with brominated radical anions relative to that of the parent structure are explained by scission of the carbon–halogen bond.

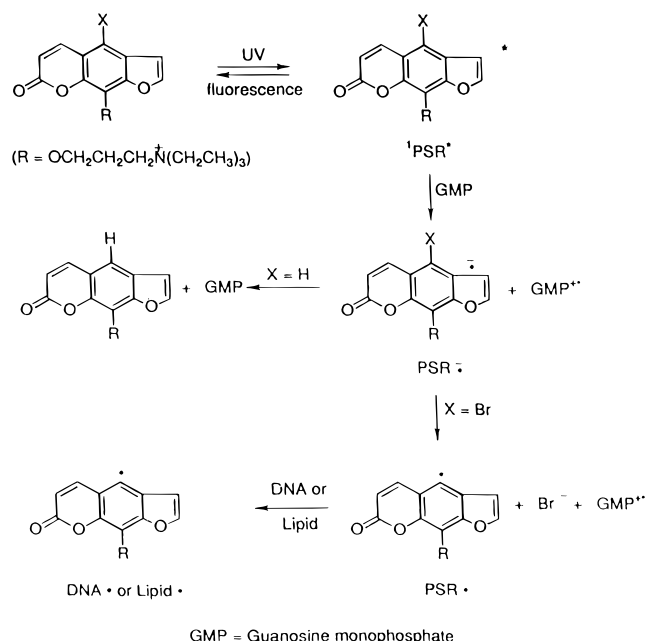
Introduction

5-Bromo-8-alkoxyypsoralens (**1a,b**) have been used as sensitizers of viral inactivation.¹ Despite improvements in serological testing and the interviewing of potential donors, there is a small but finite risk of viral transmission in transfusion medicine. The odds of contracting AIDS or hepatitis have been estimated at 1 in 100 000 and 1 in 6000 units of transfused blood, respectively.²



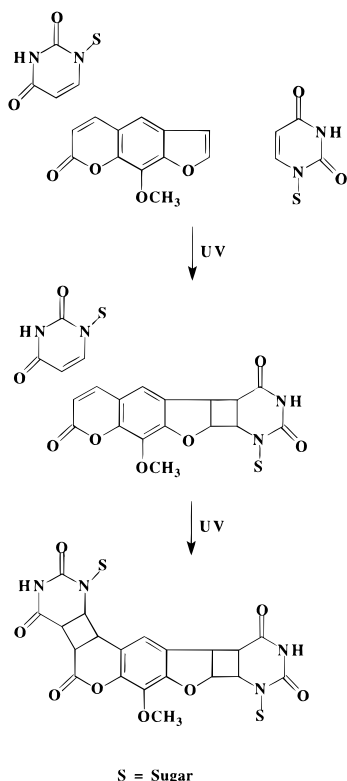
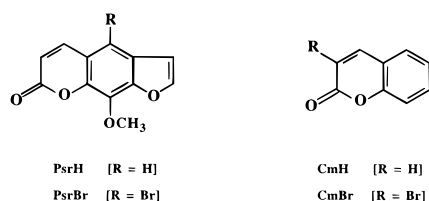
A million particles of cell-free HIV were deliberately inoculated into a full unit of platelets in a standard collection bag to simulate a worst case blood blank scenario. After addition of **1b**, the sample was exposed to 350 nm light, leading to complete inactivation of HIV with acceptable recovery of *in vitro* platelet properties.¹ This sensitizer was proposed to function by an electron transfer–free radical mechanism (Scheme 1),³ in addition to the traditional psoralen mechanism of DNA alteration by cycloaddition reactions (Scheme 2).⁴ In order to test this mechanistic design, we investigated the radical

SCHEME 1: Lighted-Induced Electron Transfer and Fluorescence Quenching of Brominated Psoralens by Guanosine Monophosphate (GMP)



anion chemistry of some psoralen and coumarin derivatives (Scheme 3) by means of electrochemical reduction of the

[®] Abstract published in *Advance ACS Abstracts*, February 15, 1997.

SCHEME 2: Consecutive Cycloaddition Reactions of 8-Methoxypsoralen to Two Uracil Derivatives**SCHEME 3: Psoralen and Coumarin Derivatives Investigated**

substrates at glassy carbon electrodes in acetonitrile and DMF, by steady-state radiolysis in 2-methyltetrahydrofuran (2-MeTHF) and in a freon matrix at 77 K, and by pulse radiolysis at ambient temperatures (in 2-methyltetrahydrofuran, alcohol, and acetonitrile). Attempts have been made to generate the corresponding aromatic radical anions and characterize them in terms of their spectroscopy, kinetics, and thermodynamics. Finally, the complete reduction mechanism upon electron transfer is presented.

Experimental Section

Materials. The syntheses of 5-bromo-8-methoxypsoralen and 3-bromocoumarin have been reported.^{1a,5} For the electrochemical investigation, acetonitrile (Merck Uvasol) and DMF (Fluka) were used as received. The supporting electrolyte, *n*-Bu₄NBF₄ (Fluka, puriss), was used as received.

Apparatus. *Electrochemical Experiments.* Most of the cyclic voltammetric experiments were carried out with a 3 mm diameter glassy carbon disk. At the highest scan rates investigated with this electrode material (100–1500 V/s), a 0.25 mm disk was used. In the high scan rate experiments we used a 10-μm-diameter carbon disk. Experiments were performed in a conventional electrochemical cell designed for use on a vacuum line, the solution volume being 5 or 10 mL. Unless otherwise indicated, positive currents are cathodic. The electrodes were carefully polished and ultrasonically rinsed with ethanol before each run. The counter electrode was a platinum wire and the reference electrode an aqueous saturated calomel

electrode (SCE). The potentiostat, equipped with a positive feedback compensation and current measurer used at low or moderate scan rates, was the same as previously described.^{6a} The instrument used with ultramicroelectrodes at high scan rates has been described elsewhere.^{6b}

Pulse Radiolytic Experiments. A detailed description of the pulse radiolytic system is given elsewhere.⁷ Steady-state spectra of radical anions were obtained in 2-methyltetrahydrofuran (2-MeTHF) glass at 77 K by following a known procedure.⁸ Methods of generation and characterization of radical ions in low-temperature matrices and the advantages of steady-state and pulse radiolysis in the application to studies of low-barrier isomerization processes in radical ions have been recently reviewed.⁹

Low-Temperature Radical Ion Spectroscopy. The spectra of the radical cations were obtained after 0.5 Mrad γ-irradiation of ~0.005 M solutions of **PsrH** or **PsrBr** in a 1:1 mixture of CF₃Cl and CF₂BrCF₂Br¹⁰ at 77 K. In the case of the radical anions, the solvent was 2-methyltetrahydrofuran (2-MeTHF). Details of the technique have been described previously.¹¹

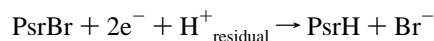
Calculations. The excited states of **PsrH**^{•+} and **PsrH**^{•-} were calculated at AM1-optimized¹² geometries by the INDO/S-CI method^{13a} (based also on ROHF wave functions^{13b}) with the ZINDO program.^{13c}

Results and Discussion

1. Electrochemical Experiments. Most of the cyclic voltammetric experiments were carried out at 293 K at a glassy carbon disk electrode which appeared, among other materials, as the best approximation of an outer sphere electron donor, i.e., of an inert electrode. As solvents, we used acetonitrile (ACN) or *N,N*-dimethylformamide (DMF) with 0.1 M *n*-Bu₄NBF₄ as supporting electrolyte (no significant difference was observed between these two solvents). The results reported below are those obtained in ACN with the psoralens and in DMF with the coumarins.

Figure 1 shows typical cyclic voltammograms of psoralens **PsrBr** and **PsrH** at low scan rates. With the halogenated **PsrBr** compound, a first irreversible two electron¹⁴ wave is located at -1.51 V vs SCE (at 0.1 V s⁻¹), and a second slightly reversible wave (with a height in between that of one and two electrons¹⁴) is found at -1.79 V vs SCE (*v* = 0.1 V s⁻¹). With **PsrH**, there is a single monoelectronic irreversible wave at the same potential as the second wave of **PsrBr**.

Therefore, the C–Br bond is cleaved during the first reduction wave of **PsrBr**, yielding a neutral radical that accepts a second electron to give a carbanion. This species is converted into **PsrH** through protonation with residual water. The expulsion of the bromide anion is demonstrated by its irreversible anodic wave, observed at +0.85 V vs SCE.



The difference in reversibility of the second wave of **PsrBr** and the single wave of **PsrH** may be due to protonation. Protonation is probably responsible for the instability of **PsrH**^{•-}. As protons are consumed in the electrode vicinity during the first reduction of **PsrBr**, the resulting less acidic medium leads to partial reversibility of the second wave of **PsrBr**.

Let us now focus on the first reduction wave of **PsrBr**. As previously shown,¹⁵ the first electron transfer may be dissociative (pathway a), which means that charge transfer and cleavage of the C–Br bond are concerted, or electron transfer and scission of the bond are two successive steps (pathway b + c: sequential mechanism). In the latter case, the additional charge

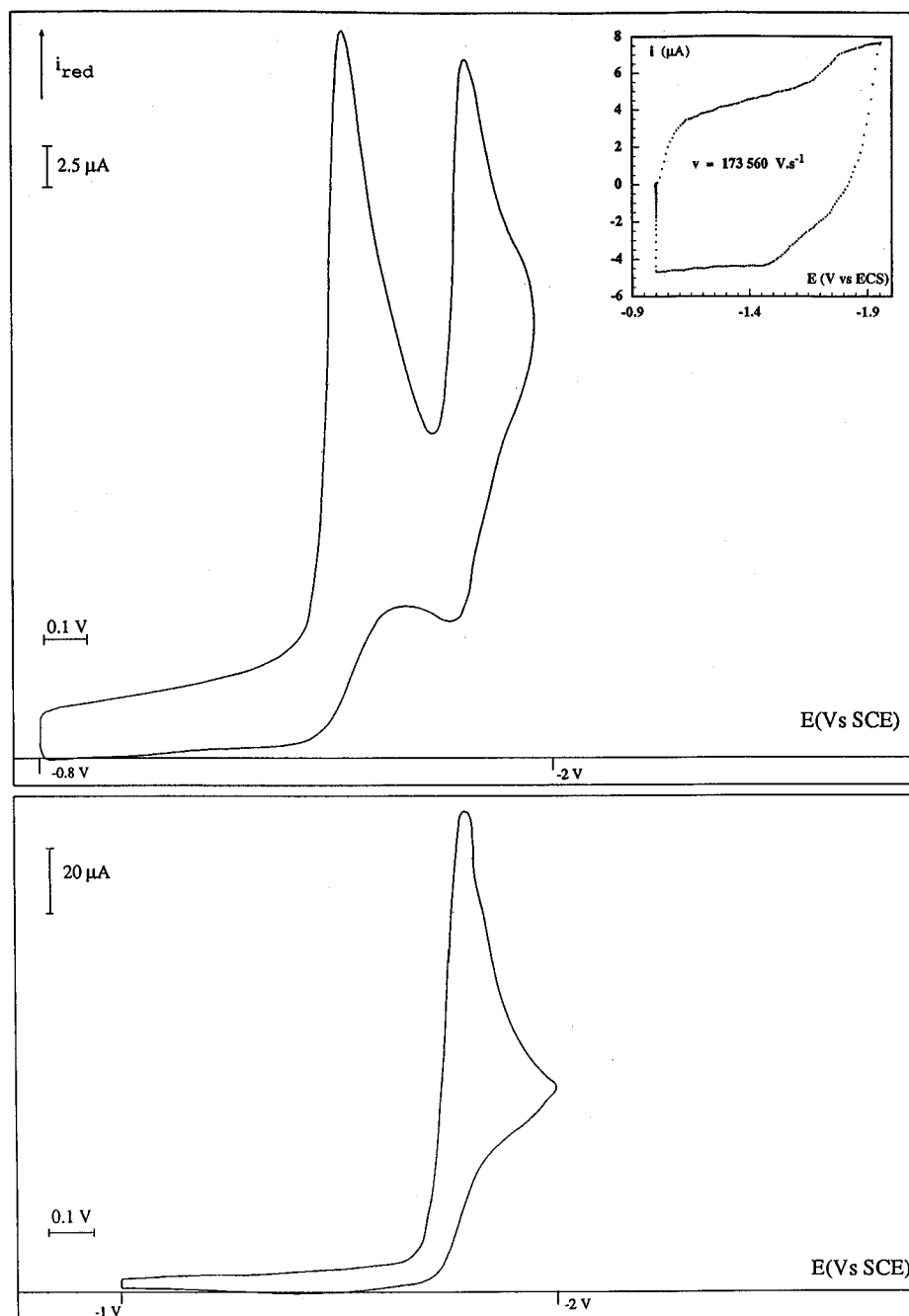
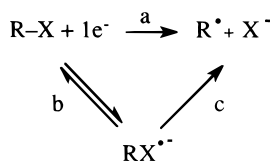


Figure 1. Cyclic voltammograms of psoralens **PsrBr** (top, $C = 0.38$ mM) and **PsrH** (bottom, $C = 2$ mM) at low scan rate (0.5 V/s). Inset: cyclic voltammetry of **PsrBr** at 173 560 V/s.

must be transiently located in a low-lying orbital such as the π^* orbital of the ring containing the carbonyl group, leading to a radical anion as a discrete intermediate.



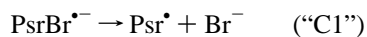
Thus, determination of the cleavage mechanism requires a closer examination of the characteristics of the corresponding cathodic peak (E_p) and peak width ($E_p - E_{p/2}$) as a function of the scan rate. The $E_p - \log \nu$ plot is linear between 0.1 and 10 V s^{-1} , with a slope close to 29 mV per unit (Table 1), the theoretical value characterizing an “E + C1” mechanism in which the rate-determining step is a first-order chemical step (“C1”) following a fast electron transfer step (“E”).^{14b,c} This

TABLE 1: Cyclic Voltammetry of PsrBr (in ACN) and CmBr (in DMF). Variations of the Peak Potential (between 0.1 and 10 V/s) and the Peak Width with the Scan Rate

	PsrBr	CmBr
$[E_{p/2} - E_p]$ mV (0.1 V s^{-1})	48	60
(1 V s^{-1})	50	65
(10 V s^{-1})	53	67
$[dE_p/d \log \nu]$ mV	29	38

is confirmed by the fact that the peak width is also almost constant (Table 1) with a value close to the theoretical value, 47 mV, characteristic of the same mechanism and kinetic situation.^{14b,c} We may then conclude that the reduction of **PsrBr** follows a stepwise mechanism. The first electron transfer leads to a radical anion as an intermediate, and then a secondary cleavage of the C–Br bond ensues with expulsion of a bromide anion and formation of an aryl radical (and these conclusions are not surprising since it has been shown that all bromoaromatic

compounds investigated so far follow the same reduction mechanism^{15f}).

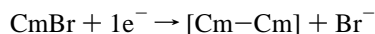


These conclusions are further confirmed by the observation that using an ultramicroelectrode of 10- μm diameter (see the Experimental Section), the reduction wave starts showing chemical reversibility above 130 000 V s^{-1} (see Figure 1). This corresponds to a lifetime of approximately 400 ns for the radical anion, with a standard potential for its formation of -1.64 V vs SCE (as determined by half the sum of the reduction and oxidation peak values). Therefore, the small distance separating the two reduction waves was itself indicative of the stepwise character of the reductive cleavage.

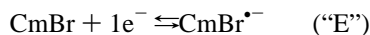
Figure 2 shows typical cyclic voltammograms of **CmBr** and **CmH** at low scan rates. With **CmBr**, a first irreversible monoelectronic¹⁴ wave is located at -1.35 V vs SCE (0.1 V s^{-1}) and a second irreversible wave (one electron¹⁴) at -1.68 V vs SCE ($\nu = 0.1 \text{ V s}^{-1}$). With **CmH**, there is a single one-electron irreversible wave at the same potential as the second wave of **CmBr**.¹⁶ Thus, the C-Br bond is cleaved during the first wave of **CmBr**, yielding a neutral radical that may abstract a hydrogen atom from the solvent to give **CmH** or dimerize, or is reduced to the anion **Cm⁻** that gives a dimer through nucleophilic attack on a **CmBr** molecule.¹⁷ Once again, formation of the bromide anion is demonstrated by the observation of its oxidation wave at positive voltage.



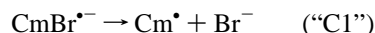
and/or



Let us now focus on the first reduction wave of **CmBr** and the mechanism it follows. The $E_p - \log \nu$ plot is linear between 0.1 and 10 V s^{-1} , with a slope close to 38 mV per unit, and the peak width ($E_p - E_{p/2}$) ranges from 60 ($\nu = 0.1 \text{ V s}^{-1}$) to 67 mV ($\nu = 10 \text{ V s}^{-1}$) (see Table 1). These values remain much below that of a rate-determining electron transfer step with a transfer coefficient of 0.5, 94 mV,^{14b,c} indicating that an "E + C1" mechanism is still operative, even if the electron transfer step participates more significantly in the mixed control of the kinetics than with **PsrBr**, as indicated by the larger waves and the bigger slope of the $E_p - \log \nu$ plot. One reason is that electron transfer itself is slower in coumarins than in psoralens because the charge is spread over a smaller volume in the former case, and thus the solvent reorganization energy is greater. A second reason is that the cleavage rate constant may be larger.



For the bromocoumarin, no chemical reversibility of the cyclic



voltammetric wave was detected up to 76 600 V s^{-1} (the highest scan rate that we were able to reach), implying that the lifetime of the radical anion is less than 650 ns.

The fact that both brominated psoralen and coumarin derivatives follow a stepwise mechanism may be understood on the basis of Savéant's dissociative electron transfer model.^{15a,18} The two main structural factors which determine the mechanism are the strength of the bond being broken and the energy of the LUMO orbital. The weaker the bond and the higher the LUMO, the more likely the concerted mechanism will be followed than

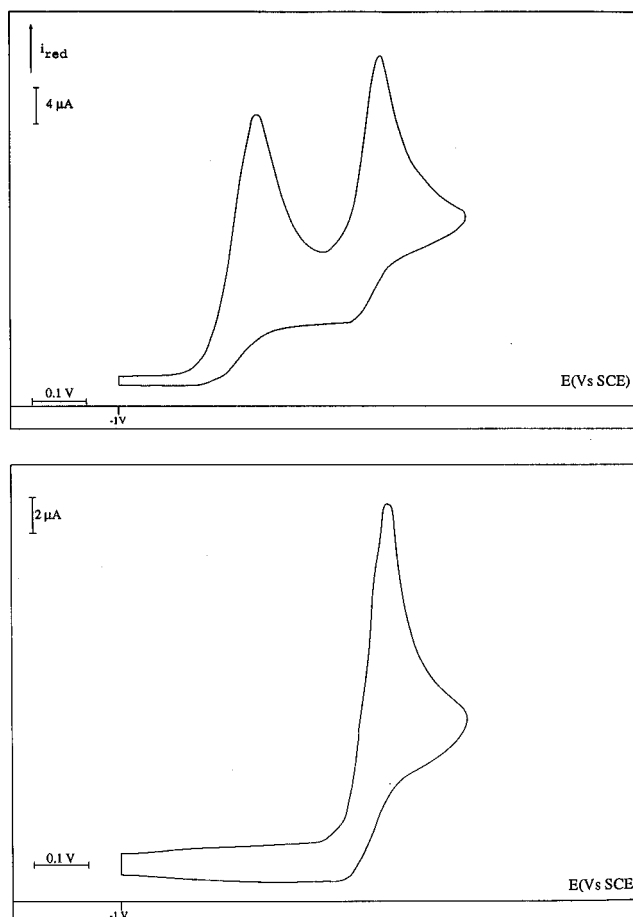


Figure 2. Cyclic voltammograms of coumarins **CmBr** (top, $C = 0.92 \text{ mM}$) and **CmH** (bottom, $C = 0.56 \text{ mM}$) at low scan rate (0.1 V/s).

the stepwise mechanism.¹⁵ Since aromatic carbon-bromine bonds are quite strong ($\sim 80 \text{ kcal/mol}^{19}$) and as the π^* orbital is delocalized on the carbonyl group and the aromatic structure (*vide infra*), there is a low well for accommodating the additional charge. In this case, the two-step pathway has a lower activation energy and thus is followed.

2. Excited states of Psoralen radical ions. Figure 3 depicts the spectra of the radical cations (lower panels) and radical anions (upper panels) of **PsrH** and **PsrBr** obtained by γ -irradiation in a mixture of freons or 2-MeTHF, respectively. The spectra obtained from the two compounds are very similar in both cases except for the shoulder at about 460 nm in the radical cation spectrum of **PsrBr** which we ascribe to an unidentified side product of the radiolysis. The spectra of the radical anions are qualitatively compatible with those obtained in aqueous solution by Bensasson et al.,^{20a} although the weak double-humped band around 600 nm was not unambiguously detected in that study. Conversely, the radical cation spectra are quite different from those ascribed to the same species by Bensasson et al. who show no trace of the structured peaks between 500 and 700 nm. As will be shown, our spectra are in reasonable accord with theoretical expectations so that we believe that those of Bensasson et al.^{20a} must be due to some other species.

Figure 4 shows a graphical representation of the results of INDO/S calculations on the excited states of **PsrH⁺** and **PsrH⁻**. There, the columns labeled "configurations" show the energies of the one-electron wave functions obtained by the electron promotions indicated above the bars, where the numbers i refer to the MO's π_i (solid bars represent excitations into the SOMO, open bars excitations into virtual MO's). These configurations combine in a configuration interaction (CI) to form the many-electron state wave functions whose energies

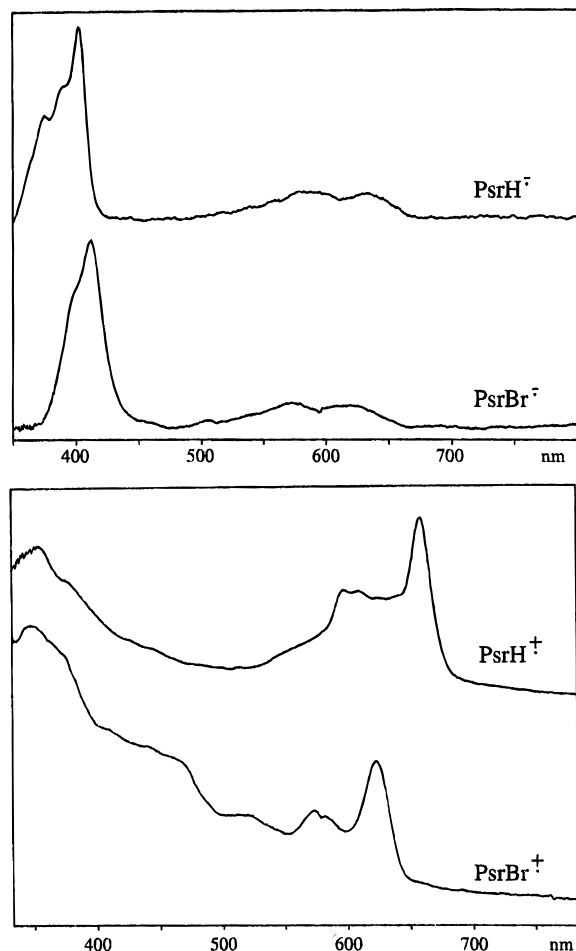


Figure 3. Spectra of the **PsrBr** and **PsrH** radical cations in a freon glass (lower panel) and of the corresponding radical anions in 2-MeTHF (upper panel), both generated by γ -radiolysis at 77 K.

are plotted in the central columns. The numbers in parentheses are the oscillator strengths for electronic transitions from the ground state whose energy was assigned a zero value. The dashed lines indicate which configurations contribute mainly to which final states. Finally, the calculated excited-state energies are juxtaposed to those obtained from the spectra in Figure 3 (columns labeled "EAS").

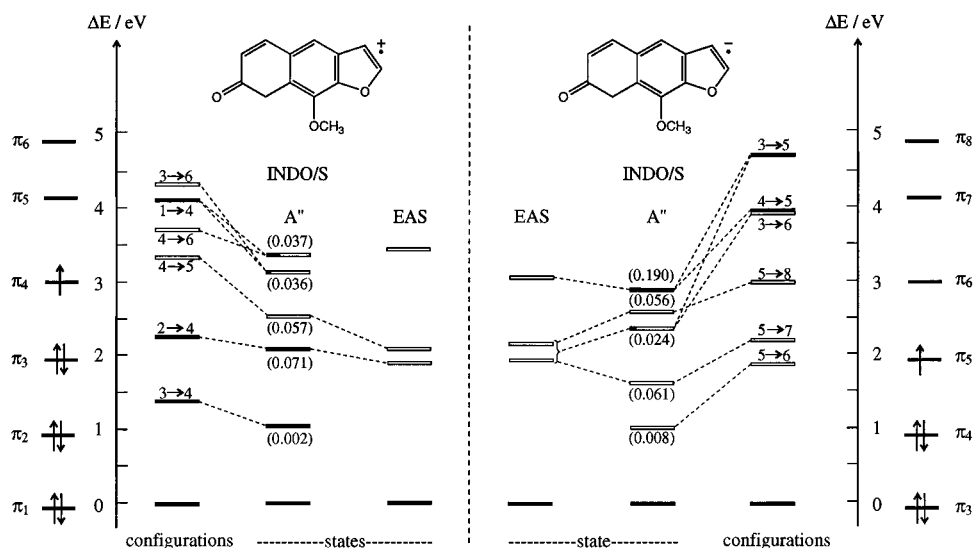


Figure 4. Graphical representation of the results of INDO/S excited-states calculations for **PsrH** $^{\bullet+}$ (left side) and **PsrH** $^{\bullet-}$ (right side). Columns labeled "configurations" represent relative energies of excited configurations attained by one-electron promotion between the MOs π_i indicated on the left and right (solid bars correspond to excitation into the SOMO, open bars to excitation into virtual MOs). Configurations combine to form states along the dashed lines. Numbers in parentheses denote oscillator strengths for one-photon excitation. The central columns represent experimental EA band positions (cf. Figure 3).

Although quantitative accord with the latter is imperfect, the calculations still yield some useful insight: they show that the observed visible bands do not correspond to the lowest excited states, but that there should be additional albeit very weak transitions in the NIR spectral region which correspond essentially to SOMO \rightarrow LUMO promotion in both cases. On the other hand, they suggest that the first absorption band of both radical ions between 500 and 700 nm is composed of excitations into two states which are, however, of very different nature (i.e., involve different MO's) in both cases.

In agreement with experiment, INDO/S predicts weak absorptions in the visible range followed by a very intense band in the near UV for **PsrH** $^{\bullet-}$. Conversely, the visible and UV bands are found to be of similar intensity in **PsrH** $^{\bullet+}$ by both experiment and calculation (the absolute intensities of the radical cation and anion bands cannot be compared due to different modes of formation). According to INDO/S the UV band of **PsrH** $^{\bullet+}$ is also composed of transitions into two excited states. This may also be the case in **PsrH** $^{\bullet-}$, but we cannot decide whether the fourth excited state predicted by INDO/S, also contributes to the broad visible absorptions. To solve these ambiguities would require more reliable *ab initio* excited-state calculations (such as CASPT2) which are, however, still prohibitively expensive for molecules of this size and low symmetry.

Nevertheless, we think that the experimental spectra conform well enough with the INDO/S predictions that the latter can be regarded as supportive of our proposed assignment of these spectra to the radical ions of the psoralens.

3. Pulse Radiolytic Experiments. Figure 5 shows electronic absorption spectra of radical anions of **PsrH**, **CmH**, and their brominated derivatives **PsrBr** and **CmBr**, obtained by pulse radiolysis (electron pulses from a linear accelerator) of the corresponding neutral precursors in a 2-methyltetrahydrofuran (2-MeTHF) matrix at 77 K. All of the radical anions possess a characteristic absorption band with maximum at 400 nm and a less intense band with $\lambda_{\max} \sim 600$ nm. No significant changes in the spectra are observed upon bromination. The radical anions observed were indefinitely stable in 2-MeTHF at 77 K. The spectra are in good agreement with the radical anion spectra obtained by γ -radiolysis.

In order to study the kinetics of the decay of these radical anions, experiments were carried out in different solvents at

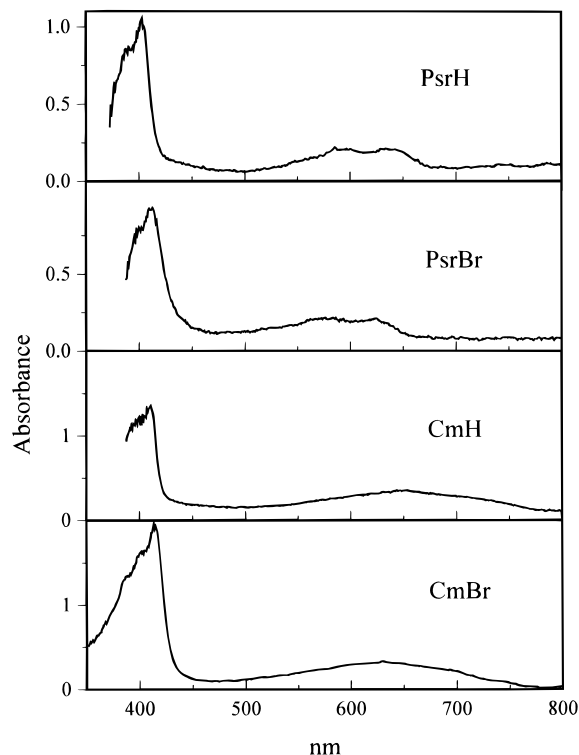


Figure 5. Steady-state spectra of radical anions of **PsrH**, **PsrBr**, **CmH**, and **CmBr** in glassy 2-MeTHF at 77 K generated by pulse electron irradiation from a linear accelerator delivering a total dose of ~ 2 kGy. Thickness of the sample = 2 mm, concentration = 0.01 M.

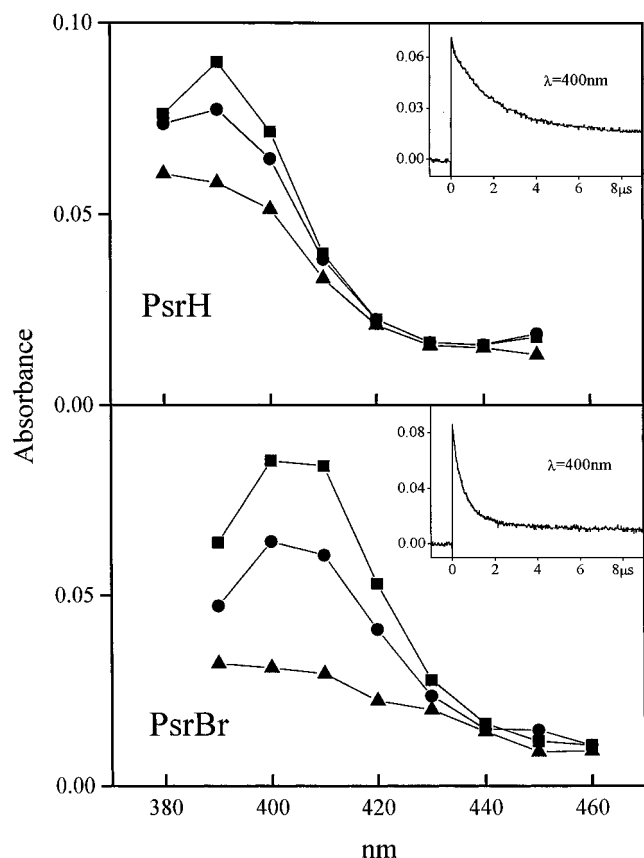


Figure 6. Time-resolved spectra of radical anions of **PsrH** and **PsrBr** in ACN generated by a 17-ns electron pulse from the linear accelerator delivering a dose of ~ 80 Gy detected 45 (■), 200 (●), and 8840 ns (▲) after the pulse. Thickness of the sample = 10 mm, concentration = 0.01 M. Insets: transient absorption decay at 400 nm.

room temperature (2-MeTHF, acetonitrile, CH_3OH , and CD_3OD). There is good agreement between spectra of radical anions

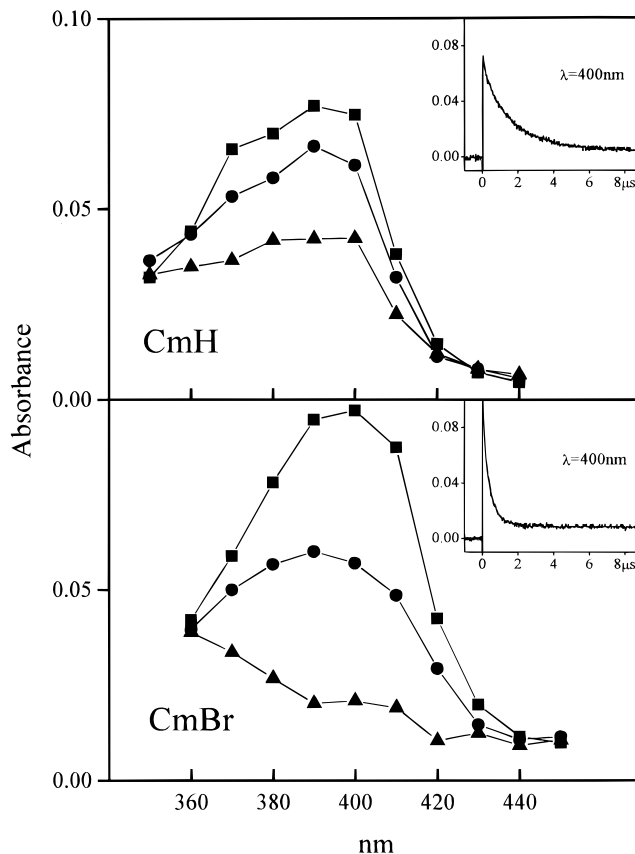


Figure 7. Time-resolved spectra of radical anions of **CmH** and **CmBr** in ACN generated by a 17-ns electron pulse from the linear accelerator delivering a dose of ~ 80 Gy detected 45 (■), 200 (●), and 8840 ns (▲) after the pulse. Thickness of the sample = 10 mm; concentration = 0.01 M. Insets: transient absorption decay at 400 nm.

TABLE 2: Radical Anion Lifetimes (ns) of $\text{PsrBr}^{\bullet-}$ and $\text{CmBr}^{\bullet-}$ Calculated from the First-Order Decays of the Transients Produced by Pulse Radiolysis

solvent	PsrBr	CmBr
2-MeTHF	280	300
ACN	590	330
CH_3OH	470	440
CD_3OD	470	450

in 2-MeTHF at room temperature and those obtained in 2-MeTHF at 77 K. However, comparison of the spectra detected at different times after the electron pulse shows that in liquid 2-MeTHF both $\text{CmH}^{\bullet-}$ and $\text{CmBr}^{\bullet-}$ are produced along with another unidentified transient absorbing on the short wavelength side of the bands of $\text{CmH}^{\bullet-}$ and $\text{CmBr}^{\bullet-}$.²¹ The transient spectra obtained in acetonitrile (ACN) are presented in Figures 6 and 7. In this case the irradiation of the precursors resulted only in the observation of the radical anions. Pulse radiolysis in alcohol solvent (CH_3OH and CD_3OD) produces the radical anions only in the case of the brominated derivatives, and the radical anion bands are blue shifted as compared to those observed in 2-MeTHF and ACN. In addition to $\text{PsrBr}^{\bullet-}$ and $\text{CmBr}^{\bullet-}$, another transient absorbing at shorter wavelength is observed. One may note that in the case of **PsrH** and **CmH** only the short wavelength transient is produced in alcohol.

The kinetics of the decay of the radical anions was monitored using the short wavelength absorption band (insets in Figures 6 and 7). For the brominated derivatives the decay follows first-order kinetics in all solvents studied and the lifetimes obtained are presented in Table 2. The decay of $\text{PsrH}^{\bullet-}$ and $\text{CmH}^{\bullet-}$ is 800 and 700 ns in 2-MeTHF and 1600 and 1300 ns in ACN, respectively. It is clear that the lifetimes of $\text{PsrBr}^{\bullet-}$ and $\text{CmBr}^{\bullet-}$ are significantly shorter than those of the nonbromi-

nated derivatives in ACN (such a comparison is not possible for radical anions generated in CH₃OH and CD₃OD; in which case only the radical anions of brominated derivatives were observed).

The fundamental reason why the lifetimes of the brominated precursors are shorter than those of the hydrogenated compounds must be the nature of the decay of the radical anions. As demonstrated by the electrochemical study, this is a first-order process involving the cleavage of the C–Br bond. It may be viewed as an intramolecular dissociative electron transfer, the additional charge temporarily located in the π^* orbital of the ring containing the carbonyl moiety being transferred to the σ^* orbital of the carbon–bromine orbital in concert with the cleavage of the bond. This type of dissociation pathway is obviously not possible in the nonhalogenated psoralens and coumarins, hence their longer lifetimes. Finally, there is satisfactory agreement between electrochemical and radiolytic measurements in the case of **PsBr**, the lifetime of the radical anion being estimated as 400 ns with the former method and 590 ns with the latter.

Conclusions

The one-electron reduction of the psoralen and coumarin derivatives involve the formation of a radical anion intermediate. The π^* orbital of the ring containing the carbonyl group provides a low-energy well where the extra electron resides. Fast electrochemical methods and pulse radiolytic generation of these intermediates demonstrate that the presence of a bromine substituent decreases the lifetime of the radical anions. This is due to C–Br bond fragmentation, leading to a bromide anion and an aryl radical. In addition to the kinetic and thermodynamic characterization of the radical anions, the electron transfer mechanism investigated here may be responsible for the improved ability of brominated psoralens to inactivate pathogenic viruses such as HIV which threatens the integrity of the blood supply. Upon UV activation, DNA-bound psoralens can be activated by UV photolysis and be reduced by an electron transfer from a guanine residue, as previously shown by fluorescence-quenching experiments.¹ The scission of a bond in the psoralen radical anion, avoiding or decreasing the yield of back electron transfer, may thus increase the effectiveness of the guanine radical cation to initiate the fragmentation process of the DNA helix.

Acknowledgment. This work was partly supported by a grant from the U.S.–Poland M. Skłodowska–Curie Joint Fund. The work in Fribourg was funded by a grant of the Swiss NSF for project No. 2028-047212.96. The authors thank Roy Williams for a sample of 3-bromocoumarin.

References and Notes

- (1) (a) Saroj, R.; Kasturi, C.; Grayzar, J.; Platz, M. S.; Goodrich, R. P.; Yerram, N. R.; Wong, V.; Goodrich, B. H. T. *Photochem. and Photobiol.* **1993**, 58, 59. (b) Goodrich, R. P.; Yerram, N. R.; Tay-Goodrich, B. H.; Forester, P.; Platz, M. S.; Kasturi, C.; Park, S. C.; Aebischer, J.-N.; Rai, S. *Proc. Natl. Acad. Sci. U.S.A.* **1994**, 91, 5552. (c) Platz, M. S.; Park, S. C.; Kasturi, C.; Rai, S.; Aebischer, J.-N.; Chen, T.; Kulaga, L.; Goodrich, R. P.; Sowemimo-Coker, S. O.; Yerram, N. R.; Tay-Goodrich, B. H.; Forster, P.; Crandall, S.; Jones, D. The Design and Development of Selective Viral Inactivation Sensitizers for Sterilization of Blood Products. In *Prevention of Transfusion Mediated Diseases*; Sieber, F., Ed.; CRC Press: Boca Raton, FL, in press.
- (2) (a) Wallace, E. L.; Surgenor, D. M.; Hao, H. S.; An, J.; Chapman, R. H.; Churchill, W. H. *Transfusion* **1993**, 33, 139. (b) Selik, R. M.; Ward, J. W.; Buchler, J. W. *Transfusion* **1993**, 33, 890. (c) Henig, R. M. In *A Dancing Matrix: Voyages Along the Viral Frontier*; A. Knopf: New York, 1993.
- (3) (a) Freeman, P. K.; Jang, J.-S.; Ramnath, W. J. *Org. Chem.* **1991**, 56, 6072. (b) Haselbach, E.; Rohner, Y.; Suppan, P. *Helv. Chim. Acta.* **1990**, 73, 1–9. (c) Nagamura, T.; Nakayama, T.; Hamanoue, K. *Chem. Lett.* **1991**, 2051.
- (4) (a) An interesting history of the use of psoralens in folk medicine can be found in the introduction of Michl, J.; Bonacic-Koutecky, V. *Electronic Aspects of Organic Photochemistry*; Wiley: New York, 1993. (b) El Mofty, A. M. *Vitiligo and Psoralens*; Pergamon: Oxford, 1968. (c) Edelson, R. L. *Sci. Am.* **1988**, 50. (d) Pathak, M. A.; Kramer, D. M.; Fitzpatrick, T. B. *Sunlight and Man*; University of Tokyo Press: Tokyo, 1974. (e) Gasparro, F. P. *Psoralen DNA Photobiology*, Vol. 1 and 2; CRC Press: Boca Raton, FL, 1988. (f) Midden, W. R. In *Chemical mechanisms of the bioeffects of furocoumarins: The role of reactions with proteins, lipids, and other cellular components, in psoralen DNA Photobiology*; Gasparro, F. P., Ed.; CRC Press: Boca Raton, FL, 1988; p 16. (g) Isaacs, S. T.; Shen, C.-K. J.; Hearst, J. E.; Rappaport, H. *Biochemistry* **1977**, 16, 1058. (h) Straub, K.; Kanne, D.; Hearst, J. E.; Rappaport, H. *J. Am. Chem. Soc.* **1981**, 103, 2347.
- (5) LeCorre, M. *Ann. Chim. (Paris)* **1968**, 3, 193.
- (6) (a) Garreau, D.; Savéant, J.-M. *J. Electroanal. Chem.* **1972**, 35, 309. (b) Garreau, D.; Hapiot, P.; Savéant, J.-M. *J. Electroanal. Chem.* **1989**, 272, 1.
- (7) (a) Karolczak, S.; Hodyr, K.; Lubis, R.; Kroh, J. *J. Radioanal. Nucl. Chem.* **1986**, 101, 177. (b) Karolczak, S.; Hodyr, K.; Polowinski, M. *Radiat. Phys. Chem.* **1992**, 3, 1.
- (8) Shida, T. *Electronic Absorption Spectra of Radical Ions*; Elsevier: Amsterdam, 1988.
- (9) Gebicki, J. *Pure Appl. Chem.* **1995**, 67, 55.
- (10) (a) Sandorfy, C.; *Can. J. Spectrosc.* **1965**, 85, 10. (b) Grimison, A.; Simpson, G. A. *J. Chem. Phys.* **1968**, 72, 1776.
- (11) (a) Bally, T. *Radical Ionic Systems*; Kluwer Academic Press: Dordrecht, 1991; Chapter 1. (b) Shida, T.; Haselbach, E.; Bally, T. *Acc. Chem. Res.* **1984**, 17, 180.
- (12) Dewar, M. J. S.; Zebisch, E. G.; Healy, E. F.; Stewart, J. J. P. *J. Am. Chem. Soc.* **1985**, 107, 3902.
- (13) (a) Zerner, M. C.; Ridley, J. E. *Theor. Chim. Acta* **1973**, 32, 111. (b) Edwards, W. D.; Zerner, M. C. *Theor. Chim. Acta* **1987**, 72, 347. (c) Zerner, M. C. *Quantum Theory Project*; University of Florida, Gainesville; program available from the author upon request.
- (14) (a) The electron stoichiometry was determined by reference to the one-electron reversible wave of benzophenone [$i_p = 0.446FSC^0D^{1/2}(Fv/RT)^{1/2}$] taking into account that the wave is irreversible [$i_p = \Psi_p FSC^0D^{1/2} (Fv/RT)^{1/2}$] with a Ψ_p coefficient that is derived from the peak width.^{14b,c} i_p is the peak current, E_p and $E_{p/2}$ are the peak and half-peak potentials, respectively, S is the electrode surface area, C^0 is the substrate concentration, D is its diffusion coefficient, and v is the scan rate. (b) Andrieux, C. P.; Savéant, J.-M. In *Electrochemical Reactions, Investigation of Rates and Mechanisms of Reactions, Techniques of Chemistry*; Bernasconi, C. F., Ed.; Wiley: New York, 1986; Vol. VI/4E, Part 2, pp 305–390. (c) Nadjio, L.; Savéant, J.-M. *J. Electroanal. Chem.* **1973**, 48, 113.
- (15) (a) Savéant, J.-M. Dissociative Electron Transfer. In *Advances in Electron Transfer Chemistry*; JAI Press: New York, 1994; Vol. IV, pp 53–116. (b) Andrieux, C. P.; Le Gorand, A.; Savéant, J.-M. *J. Am. Chem. Soc.* **1992**, 114, 6892. (c) Andrieux, C. P.; Differding, E.; Robert, M.; Savéant, J.-M. *J. Am. Chem. Soc.* **1993**, 115, 6592. (d) Andrieux, C. P.; Robert, M.; Saeva, F.; Savéant, J.-M. *J. Am. Chem. Soc.* **1994**, 116, 7864. (e) Savéant, J.-M. *Acc. Chem. Res.* **1993**, 26, 455. (f) Savéant, J.-M. *Adv. Phys. Org. Chem.* **1990**, 26, 1. (g) For related gas phase work, see: Bulliard, C.; Allan, M.; Haselbach, E. *J. Phys. Chem.* **1994**, 98, 11040.
- (16) As with **PsH**, irreversibility of the reduction wave is probably due to a fast chemical reaction following the charge transfer ($E + C$ mechanism) as indicated by its characteristics ($E_p - E_{p/2} \approx 50$ mV, $[dE_p/d \log v] \approx 24$ –25 mV). This reaction could be a protonation or a protonation coupled with a dimerization or even a dimerization since peak potential is concentration dependent ($[dE_p/d \log v] \approx 16$ mV). Due to this irreversibility, the lifetime of the radical anion could not be deduced.
- (17) Even if the dimer **Cm–Cm** is the final product of reduction rather than **CmH**, these two molecules may have very similar reduction potentials. The fact that the reduction wave of **CmBr** is mono-electronic and that of **PsBr** is bi-electronic is certainly related to the more positive reduction potential of the former compound as compared to the latter (~ 160 mV), giving rise to a more stable **Cm** radical that may undergo chemical reaction prior to immediate reduction into an anion.
- (18) (a) Savéant, J.-M. *J. Am. Chem. Soc.* **1987**, 109, 6788. (b) Savéant, J.-M. *J. Am. Chem. Soc.* **1992**, 114, 10595.
- (19) (a) Griller, D.; Kanabus-Daminska, J. M. In *Handbook of Photochemistry*, Vol. 2; Scaiano, J. C., Ed.; CRC Press: Boca Raton, FL, 1989; pp 359–362.
- (20) (a) Bensasson, R. V.; Chalvet, O.; Land, E. J.; Ronfard-Haret, J. C. *Photochem. Photobiol.* **1984**, 39, 287. (b) Bensasson, R. V.; Land, E. J.; Salet, C.; Sloper, R. W.; Truscott, T. G. In *Radiation Biology and Chemistry: Research Developments*; Edwards, H. E.; Navaratnam, S.; Parsons, B. J.; Phillips, G. O., Eds.; Elsevier: Amsterdam, 1979; pp 431–439. (c) Bensasson, R. V.; Land, E. J.; Truscott, T. G. *Flash Photolysis and Pulse Radiolysis*; Pergamon Press: Oxford, U.K., 1983; pp 200–204.
- (21) These unidentified transients decay slower than **CmH[•]** and **CmBr^{•-}**. The responsible species are not formed directly from the corresponding radical anions but may be due to reaction of products of the radical anion decay or to byproduct of radiolysis.